J Atmos Chem (2010) 66:137–155
DOI 10.1007/s10874-011-9197-y

Detection of radical species formed by the ozonolysis of α-pinene

Jelica Pavlovic · Philip K. Hopke

Received: 13 November 2010 / Accepted: 4 August 2011 /
Published online: 3 September 2011

Abstract Highly reactive free radical species have been subject of many toxicological in vivo and in vitro studies because of the oxidative cell damage they cause. Similar species have been postulated to be the key intermediates formed during many environmental chamber reactions and atmospheric oxidation of organic species present in the troposphere. Thus, detection and characterization of these transient radical species are important steps in understanding the atmospheric chemistry and confirming the reaction pathways involved in secondary organic aerosol formation. Study of these species is particularly difficult because of their short life-times. To facilitate such studies, 5,5-dimethyl-1-pyrroline-N-oxide (DMPO) and diethyl-(2-methyl-1-oxido-3,4-dihydro-2H-pyrrol-2-yl) phosphonate (DEPMPO) nitrone spin traps were used to capture radicals formed from the α-pinene/ozone reaction. Electrospray ionization/tandem mass spectrometry (ESI/MS^n) was applied to elucidate their structures. Characteristic fragments with m/z 114, m/z 130 and m/z 148 with the DMPO trap, and m/z 236, m/z 252, and m/z 270 with the DEPMPO trap indicated the existence of alkyl, alkoxyl and peroxyl radicals, respectively.

Keywords Reactive oxygen species · Free radicals · Spin trapping · DMPO · DEPMPO

1 Introduction

Particle size and composition play important role in particulate matter toxicity. Reactive oxygen species (ROS) can be generated endogenously, after exposure and inhalation of the fine ($PM_{2.5}$) and especially the ultrafine particles (PM<0.1 μm) (Li et al. 2003a). In addition, significant amounts of ROS were measured in respirable ambient particles prior to inhalation (Venkatachari et al. 2005, 2007), as well as in the secondary organic aerosol (SOA) formed under laboratory conditions during the monoterpene/O_3 reaction (Venkatachari and Hopke 2008; Chen and Hopke 2009a, 2009b, 2010).

J. Pavlovic · P. K. Hopke (✉)
Center for Air Resources Engineering and Science, Clarkson University, Potsdam, NY 13699-5708, USA
e-mail: hopkepk@clarkson.edu

ROS can cause oxidative stress that result in damage of cellular membranes, DNA and proteins, and may exacerbate many inflammatory effects, such as asthma, chronic bronchitis, ischemic heart disease, stroke, etc. (Delfino et al. 2005; Dreher and Junod 1996; Li et al. 2003b). Epidemiological studies have linked $PM_{2.5}$ and ultrafine particles (UFPs) to cardiovascular diseases and airborne pollutants to many respiratory outcomes (Pope et al. 2002; Pope and Dockery 2006). There is increasing evidence that products of reactions between ozone and compounds with unsaturated C-C bonds in indoor environments are associated with "sick-building syndrome" (SBS) symptoms, including eye and upper airway irritation (Wolkoff et al. 1997). Among the different classes of ROS are also highly reactive radical species formed during the ozonolysis of monoterpenes.

Chen and Hopke (2010) measured short-lived, highly reactive fraction of the ROS from the limonene/ozone reaction, as the fraction of ROS that was lost when samples were stored for 24 h in a freezer. That fraction was found to account for up to 17% of the total ROS measured immediately after the collection. The estimated ROS half-life time was approximately 6.5 h at room temperature (Chen et al. 2011) for the same reaction. Time sensitivity of ROS reflects the significance of these short-lived species and the need to overcome present technical limitations of sampling methods and analysis.

Reactive radical species represent one part of the ROS, but previous studies identified only hydroxyl (OH) radicals (Aschmann et al. 2002; Atkinson et al. 1995) from the monoterpene/ozone reaction. Short-lived free radical species include inorganic hydroxyl (OH) and hydroperoxyl (OOH) radicals, and organic radicals such as alkyl (R), alkoxyl (RO), and peroxyl (ROO) radicals. Besides the direct adverse health effects that radicals can cause, these compounds can be involved in the formation of first stage oxidation products (monomers) and it is hypothesized that radicals can also be involved in the formation of higher molecular weight species - oligomers (Hallquist et al. 2009).

The specific objectives of the present research were to develop a method to detect and identify different classes of radical species from the α-pinene/ozone reaction, and to apply that method to confirm the hypothesized reaction pathways. Spin trapping is an analytical method employed in the detection and characterization of free radicals. Unstable free radical species react with a diamagnetic molecule (the spin trap) and form more stable free radical – spin trap adducts. The most frequently used spin traps are nitrone spin traps and those spin traps (5,5-dimethyl-1-pyrroline-N-oxide (DMPO) and diethyl-(2-methyl-1-oxido-3,4-dihydro-2H-pyrrol-2-yl) phosphonate (DEPMPO)) were used in the present study as well, to capture radicals formed from the α-pinene/ozone reaction.

Electrospray Ionization (ESI) tandem mass spectrometry (MS^n) was used to elucidate the characteristic decomposition pathways of DMPO and DEPMPO adducts, and to identify nature of detected radicals, i.e. possible location of the spin (oxygen- versus carbon-centered radicals). The chemical structures of detected radical species were tentatively identified based on these results and the existing knowledge about the chemical composition of the organic aerosols derived from the α-pinene/O_3 reaction.

2 Experimental procedures

The reaction of α-pinene and O_3 was performed in the dark in a Pyrex flow reactor (Venkatachari and Hopke 2008). The length of the reactor was 120 cm (900 mm I.D.) and the volume 7.7 L. The residence time of the reactants in the chamber was 3.85 min. No HO· scavengers were used. Experiments were carried out at 296±2 K and relative humidity between 5 and 30%. Monoterpene vapor was produced by passing ultra high purity

(99.999%) nitrogen through a midget impinger (25 ml) filled with α-pinene liquid (98% purity, Sigma Aldrich, USA). The vapor was then introduced into the reactor with at a flow rate of 0.5 LPM. The resulting concentration of α-pinene was relatively constant between 2.5 and 3.0 ppmv for all of the experiments. The concentration of α-pinene entering the reactor was sampled with a gas tight syringe and analyzed by gas chromatography-flame ionization detection (GC-FID; Thermo Finnigan, USA). Ozone was generated with an "Ozone Purification" system (Air Zone, VA, USA). The ozone was introduced into the reactor at a flow rate of 1.5 LPM with the resulting concentration of 2.5 to 3.0 ppmv. Room air was used for the ozone generator after it passed through a high-efficiency particulate (HEPA) filter. Unreacted ozone exiting the system was removed with a charcoal diffusion denuder. The α-pinene oxidation products exiting the denuder were collected at a final flow rate of 2 LPM.

Particulate matter samples were collected for 30 min on 25 mm pre-baked quartz fiber filters (16 h at 550°C). The filters were immediately immersed into 10 ml of HPLC water that contained either 0.5 mg of the DMPO or 0.5 mg of the DEPMPO spin trap (Alexis Biochemicals, Switzerland) and then sonicated for 10 min. Because of the air- and light-sensitivity of the reagents, all reactions were conducted in the dark and under ultrahigh purity argon in a glove bag. The filter extracts were filtered through 0.45 μm Acrodisc™ syringe filters (Pall). The resulting samples were then analyzed using a Thermo LCQ Advantage ESI/MS^n system with direct sample injection without column separation. ESI was employed in the positive (+) scan mode and the mass spectra were recorded over the mass range of m/z 100–1000. The ion optics of the ion trap mass spectrometer were optimized for the $[M+H]^+$ ion of the DMPO and DEPMPO at m/z 114 and m/z 236, respectively.

For the MS^n experiments, the applied collision energies were between 30% and 35% (100% collision energy corresponds to 5 eV) using helium as the collision gas. Ten (10) replicate samples were collected and analyzed for the same reaction and laboratory conditions. To obtain insights into possible artifacts and to eliminate them, a negative controls consisting of pre-baked quartz filters exposed to a flow of α-pinene/ozone (without nitrone) and α-pinene (without ozone) plus DMPO. These filters were then treated in the same way as the actual samples and analyzed using the same instrumental conditions.

3 Results and discussion

3.1 Blank samples

Pinene plus ozone blank samples, without DMPO trap (Fig. 1a) in the (+) ESI almost always have odd nominal masses and originate either from monomer or oligomer closed-shell molecular species. In the higher mass range (m/z>250), clusters were observed separated by 12–16 amu. Adjacent ions in the single clusters were separated by 1 amu, indicating that only single charged ions were present. Similar patterns in the ESI-QTOF mass spectrum were found by Tolocka et al. (2004) for SOA produced by the same reaction. Other ions found in the lower mass region (m/z<250) are expected to be α-pinene oxidation products containing keto, aldehyde, hydroxyl, hydroperoxyl and epoxyl functional groups, and have been identified and described in detail elsewhere (Winterhalter et al. 2003; Glasius et al. 1999).

In the mass spectrum of pinene plus DMPO blank samples (without ozone), the most intensive were the ions at m/z 114 and m/z 227 (Fig. 1b). These adducts correspond to the quasi-molecular ion $[DMPO+H]^+$ and molecular cluster $[2DMPO+H]^+$, respectively.

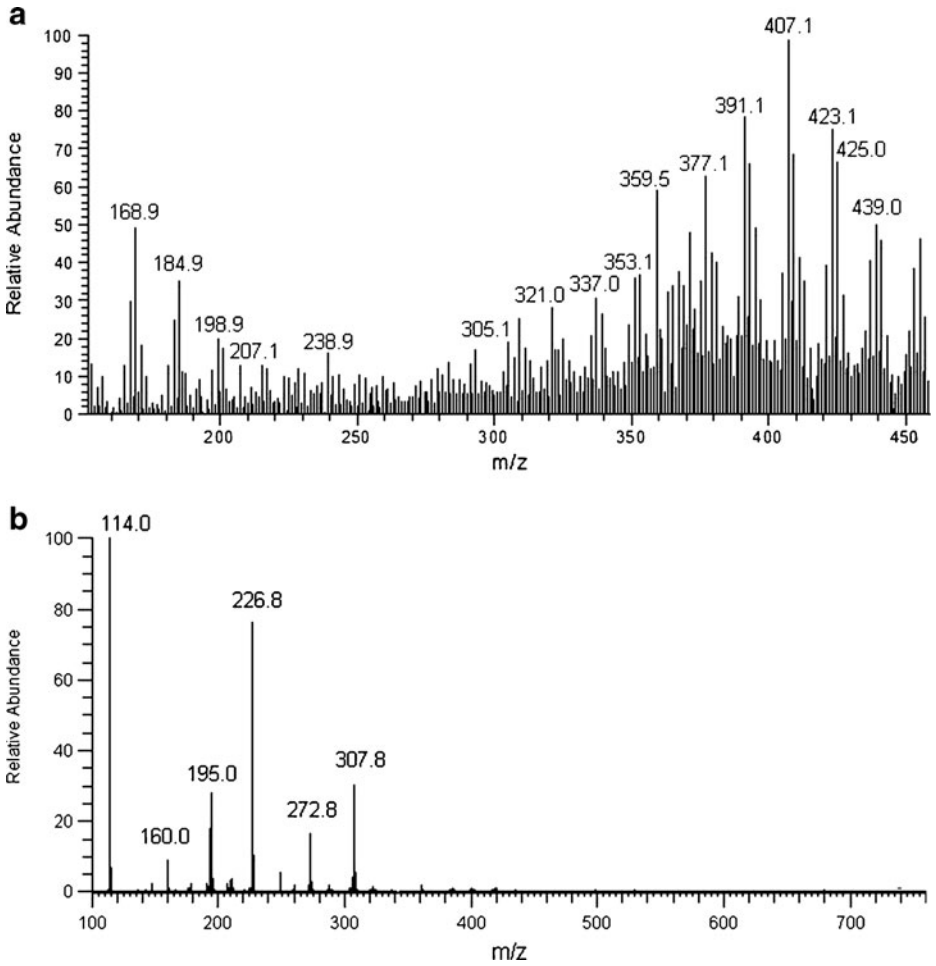

Fig. 1 Full mass spectrum of **a**) α-pinene/O_3 blank **b**) α-pinene/DMPO blank

3.2 Full MS spectrum of sample (m/z 100–350)

The average ESI (+) mass spectrum of the products formed during the α-pinene/O_3 reaction in the presence of a DMPO is displayed in Fig. 2a (m/z 100–250) and b (m/z 250–350), and in the presence of DEPMPO in Fig. 2c (m/z 220–320) and d (m/z 350–450).

In the lower mass region of the DMPO spectrum (Fig. 2a), positive ions at m/z 114, m/z 227, m/z 130, and m/z 211 dominate. From the fragmentation results, these ions were assigned to protonated DMPO, molecular cluster $[2DMPO+H]^+$, and hydroxyl radical adducts $[DMPO\text{-}OH+H]^+$, and $[2DMPO\text{-}O+H]^+$, respectively. Formation of the same ions under oxidative conditions was also observed by Domingues et al. (2001). Other ions observed in the same mass region are expected to be the first stage oxidation products of α-pinene (monomer species).

Figure 2c (m/z 220–320) shows the ions formed in the lower mass region during the reaction of α-pinene and O_3 in the presence of DEPMPO. The spectrum showed a major peak at m/z 236 as well as secondary peak at m/z 258 that can be attributed to the

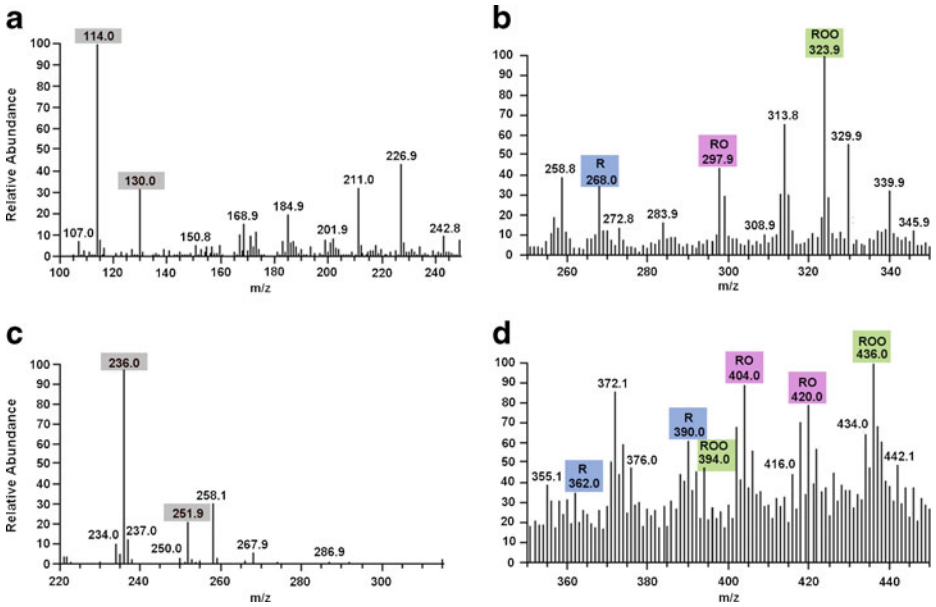

Fig. 2 Full MS of sample with DMPO (**a**) m/z range 100–250 and (**b**) m/z range 250–350 and DEPMPO trap (**c**) m/z range 220–320 and (**d**) m/z range 350–450

protonated molecule $[DEPMPO+H]^+$ and to its sodium adduct analogue $[DEPMPO+Na]^+$, respectively. The third ion observed in the spectrum has m/z 252 and, as in the case of DMPO spin adduct at m/z 130, could be formed after trapping a hydroxyl radical by DEPMPO, i.e., $[DEPMPO\text{-}OH+H]^+$. In order to confirm structure of that adduct (Scheme 1), it was submitted to fragmentation. The most abundant fragment ion present in the MS^2 spectrum had m/z 114. That ion most likely arose from the neutral loss of diethyl phosphonate molecule (−138 Da). Tuccio and coworkers (2006) reported the same fragmentation pattern (−138 Da) as a result of the MS^2 analysis of the DEPMPO and its C-centered adducts.

In the higher mass range (Fig. 2b and d), some ions were identified as the DMPO and DEPMPO adducts with carbon- and oxygen- centered organic radical species formed after α-pinene ozonolysis and will be discussed in detail later. The identified organic radicals correspond to alkyl (R), alkoxyl (RO), and peroxyl (ROO) radicals. Other ions observed in that range are possible dimer species formed as products of reactions of the first stage oxidation products (monomer species). Their MS^2 fragmentation spectra did not reveal any fragments that can be recognized as positive ions of either DMPO or DEPMPO traps, and

Scheme 1 Proposed fragmentation pathway for the transition m/z 252 → m/z 114

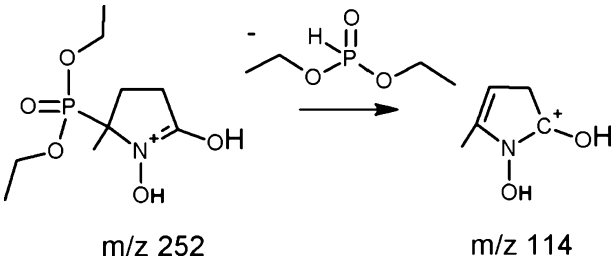

therefore, these ions were not analyzed further. The adducts formed with the DEPMPO trap had greater stability: ~30 min vs. ~15 min with the DMPO trap. In addition, the DEPMPO was able to capture more radical species that were then observed in the DEPMPO spectra.

The nitrone radical adducts can be present in the MS in three different protonated forms: oxidized, radical, and reduced, that all differ by m/z 1 (Guo et al., 2003). The structures and formation of three protonated forms of hydroxyl and hydroperoxyl adducts of DMPO is shown in the Supporting Information (Fig. 1SP). All forms are almost always present in the full MS of the samples (Guo et al. 2003; Domingues et al. 2003), but with different intensities. The blank samples (pinene + ozone, without nitrone) in the full (+) ESI/MS almost always have odd nominal masses (Fig. 1a), but originate either from monomer or oligomer closed-shell species. Therefore, the odd nominal nitrone adduct masses (radical forms) have not been analyzed by tandem MS. The even nominal masses were analyzed and some are assigned as nitrone radical adducts in reduced or oxidized forms. However, the even masses might also be attributed to molecular clusters formed during the ESI between the stable organic molecule (even mass) and the protonated nitrone ($[DMPO+H]^+$, MW=114 or $[DEPMPO+H]^+$, MW=236). Thus, the MS^n fragmentation patterns and formation of specific fragment ions that were used in previous spin trap research studies (Reis et al. 2003, 2004; Guo et al. 2003; Domingues et al. 2003), were the most informative, as they allow the proposal of the presence of carbon- and oxygen- centered adducts and even the location of the radical species within the structure. Table 1 summarizes these characteristic fingerprint fragments and ions detected and analyzed with both nitrones. Possible chemical structures (carbon skeletons and functional groups) of trapped organic radicals are proposed based on MS^n fragmentation results and available literature for the same α-pinene/O_3 reaction. The ESI/MS^n provides reasonably reliable information about functional groups and molecular masses. However, without any further identification by other techniques (higher resolution MS), the exact molecular structures (and masses) of all species proposed here remain speculative.

3.3 Alkyl radicals (R)

The ions at m/z 268 with DMPO (Fig. 2b), m/z 390 and m/z 362 with DEPMPO (Fig. 2d), were identified to result from the reaction of the spin traps with carbon-centered radicals formed from the α-pinene/O_3 reaction. The formation of carbon-centered DMPO adduct at m/z 268 is shown in Fig. 3a. That adduct ion can be the result of reaction of DMPO with molecular weight (MW) 113 Da and alkyl radicals with MW 153 Da.

The ESI (+)/MS/MS spectrum of that DMPO adduct is also shown in Fig. 3a. For identification purposes, the most important fragments are: m/z 114 (protonated molecule of the DMPO trap) and m/z 155 that correspond to the neutral loss of 113 Da, most likely due to the loss of the DMPO moiety. Proposed fragmentation mechanisms that occur in the radical part of the adduct and resulted in formation of the ions at m/z 198 and m/z 170 are illustrated in Scheme 2a–b. These fragment ions formed after the heterolytic cleavage inside of four-membered-carbon ring, and the neutral loss of C_4H_6O (−70 Da) and $C_6H_{10}O$ (−98 Da) groups, respectively, are in agreement with the suggested radical and DMPO adduct structure.

In order to gain deeper insight into the chemical structure of ion at m/z 155, MS^3 studies were performed. The MS^3 spectrum presented on Fig. 3b indicates that the most abundant product ion (m/z 137) is likely to arise by the expulsion of H_2O molecule (−18 Da) as a result of charge-remote rearrangements (Scheme 3a). The presence of a terminal carbonyl group is confirmed by the loss of C_2H_4O moiety (−44 Da) and the fragment ion at m/z 111 in the MS^3 spectrum (Scheme 3b). Heterolytic cleavage inside of four-membered ring structure resulted

Table 1 Characteristic fragment ions fund in MS^n of the nitrone (DMPO and DEPMPO) adducts

Fragment Ion									
Nitrone adducts	Nitrone used	$[N+H]^+$	$[N\text{-}OH+H]^+$	$[NOOH+H]^+$	-[N]	-[N-OH]	-[N-OOH]	- 138 Da[a]	Radical nature
m/z 130	DMPO	+	+						OH
m/z 252	DEPMPO	+	+					+	OH
m/z 268	DMPO	+			+				R
m/z 390	DEPMPO	+			+			+	R
m/z 298	DMPO	+	+			+			RO
m/z 420	DEPMPO	+	+		+			+	RO
m/z 404	DEPMPO	+	+		+			+	RO
m/z 314	DMPO	+	+	+	+				ROO
m/z 436	DEPMPO	+	+	+	+			+	ROO

+ Fragment ion present in MS^n

[a] 138 Da=diethyl phosphonate molecule (common fragment from DEPMPO nitrone)

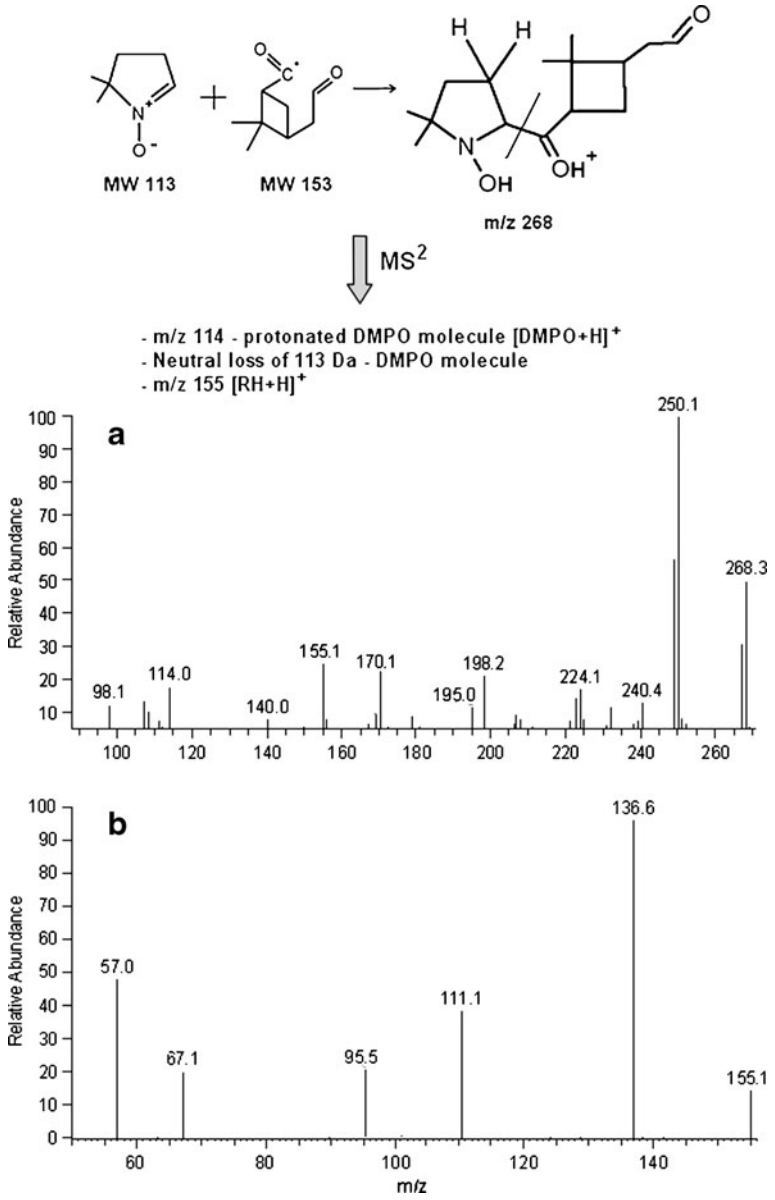

Fig. 3 **a**) Formation and MS^2 fragmentation of DMPO-alkyl adduct at m/z 268 **b**) MS^3 fragmentation of m/z 155

in the low mass fragment ion with m/z 57 (Scheme 5c). The structure of that ion enables delocalization of the positive charge and provides an explanation for its stability.

The same experimental procedure was repeated with DEPMPO and the ion at m/z 390 can be the result of reaction of the spin trap and the same alkyl radical with MW 153 Da. Another alkyl radical detected with DEPMPO has MW 125 Da and is shown in Fig. 2d as a carbon-centered adduct at m/z 362. Fragmentation of the DEPMPO-alkyl radical adducts (Supporting Information, Fig. 3SPa) occurs mainly via

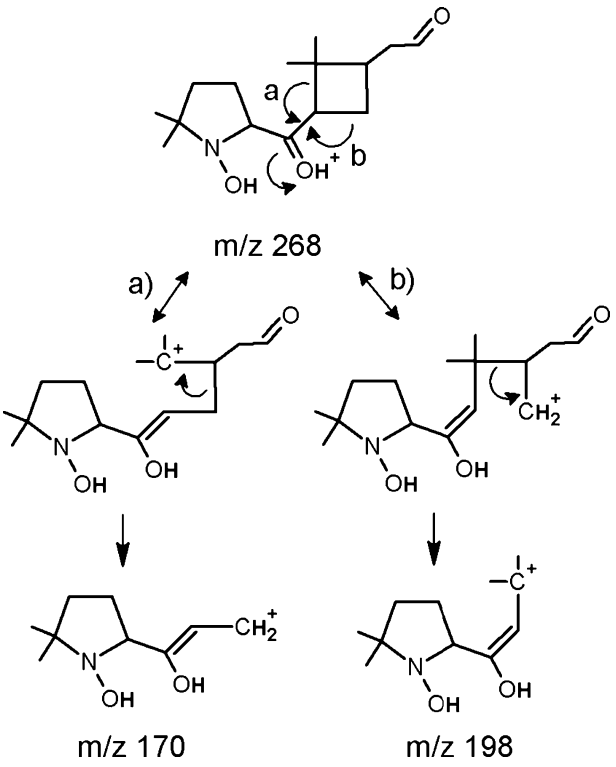

Scheme 2 Proposed fragmentation pathways for the transitions **a**) m/z 268 → m/z 170 and **b**) m/z 268 → m/z 198

the loss of a water molecule (−18 Da) and a diethyl phosphonate molecule (−138 Da). However, the presence of either the m/z 236 ion (protonated spin trap), or ion that represents the neutral loss of a DEPMPO molecule (−235 Da) in fragmentation spectra indicate the formation of DEPMPO spin trap adducts and the nature of analyzed radical species. Similar fragmentation patterns for spin trap-alkyl radical adducts were observed in previous studies (Reis et al. 2003, 2004, 2009). To further confirm the structure of alkyl radical with MW=153 Da, MS^3 experiments of the daughter ion at m/z 153 were conducted, and the resulting spectrum together with proposed fragmentation mechanisms can be found in the Supporting Information.

The identified alkyl radicals from monoterpene/ozone reaction can be formed either after H-atom abstraction from the first stage oxidation products by OH radicals or after decomposition and isomerization of alkoxyl (RO) radicals. The carbon-centered radical species are not considered to be reactive oxygen species, but their further reactions in the presence of oxygen molecule can lead to peroxyl (RO_2) radical formation. The peroxyl radical may capture H-atom by abstraction from another molecule to generate a hydroperoxide, or decompose to a corresponding alkoxyl (RO) radical.

3.4 Alkoxyl radicals (RO)

The ions at m/z 298 with DMPO (Fig. 2b), m/z 420 and m/z 404 with DEPMPO (Fig. 2d) were identified as adducts formed after the reaction of spin traps and oxygen-centered, alkoxyl (RO·) radicals. The formation of oxygen-centered DMPO-alkoxyl adduct at m/z 298 is shown in Fig. 4a together with MS^2 fragmentation spectrum of the same adduct.

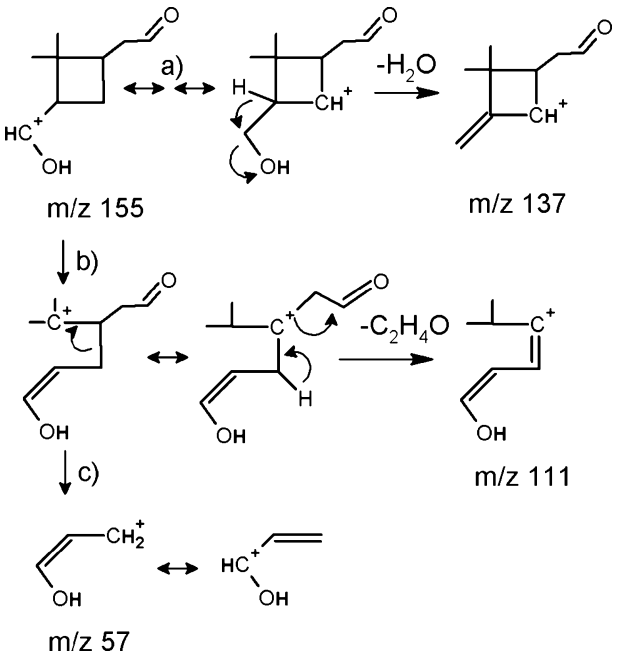

Scheme 3 Proposed fragmentation pathways for the transitions **a**) m/z 155 → m/z 137; **b**) m/z 155 → m/z 111, and **c**) m/z 155 → m/z 57

The most intense peak after MS^2 fragmentation was at m/z 114 (protonated molecule of DMPO), confirming that the analyzed ion is a spin trap adduct. The fragment at m/z 130 can be attributed to the protonated molecule of hydroxyl radical-DMPO, $[DMPO\text{-}OH+H]^+$, and is the evidence that the captured radical have alkoxyl nature. That m/z 130 ion was found as a result of ESI/MS/MS fragmentation of other DMPO adducts of oxygen-centered radicals in previous studies (Reis et al. 2003, 2004), as well.

The proposed chemical structures of that adduct and RO· radical are again the result of detailed interpretation of MS^2 spectrum of the adduct (Fig. 4a) and MS^3 average spectrum of the adduct's daughter ion at m/z 169 (Fig. 4b). The formation of that ion (m/z 169) could be the result of the neutral loss of oxidized form of the DMPO-OH molecule (−129 Da, Scheme 4).

Its structure is further confirmed by the MS^3 fragmentation (Fig. 4b). Fragments at m/z 151 and m/z 125 are formed as a result of inductive heterolytic cleavages and expulsion of H_2O and CH_2=CHOH molecules, respectively (Scheme 5). Both ions demonstrate the presence and position of the hydroxyl group in the radical structure. Formation of the ions with m/z 150 and m/z 124 can be explained by additional loss of hydrogen radicals ($-H^{\cdot}$). Inductive and α-cleavages in these structures will further lead to the formation of fragments with m/z 107 and m/z 133. In fact, the m/z 107 was the main fragment ion found in the MS^3 spectrum, probably because it can be formed from both positively charged radicals (m/z 150 and m/z 124) although with different structures.

In the presence of DEPMPO, a peak with m/z 420 was detected and most likely corresponds to the adduct formed with the same radical specie (MW=183). Fragmentation of that adduct (Supporting Information, Fig. 4SP) produce abundant fragments that represent the protonated form of spin trap molecule (m/z 236), the loss of water (−18 Da), the loss of diethyl phosphonate molecule (−138 Da), or a spin trap molecule (−235 Da). Less abundant, but more important, was the fragment at m/z 252. That ion corresponds to the protonated form of hydroxyl radical – DEPMPO adduct, $[DEPMPO\text{-}OH+H]^+$. The

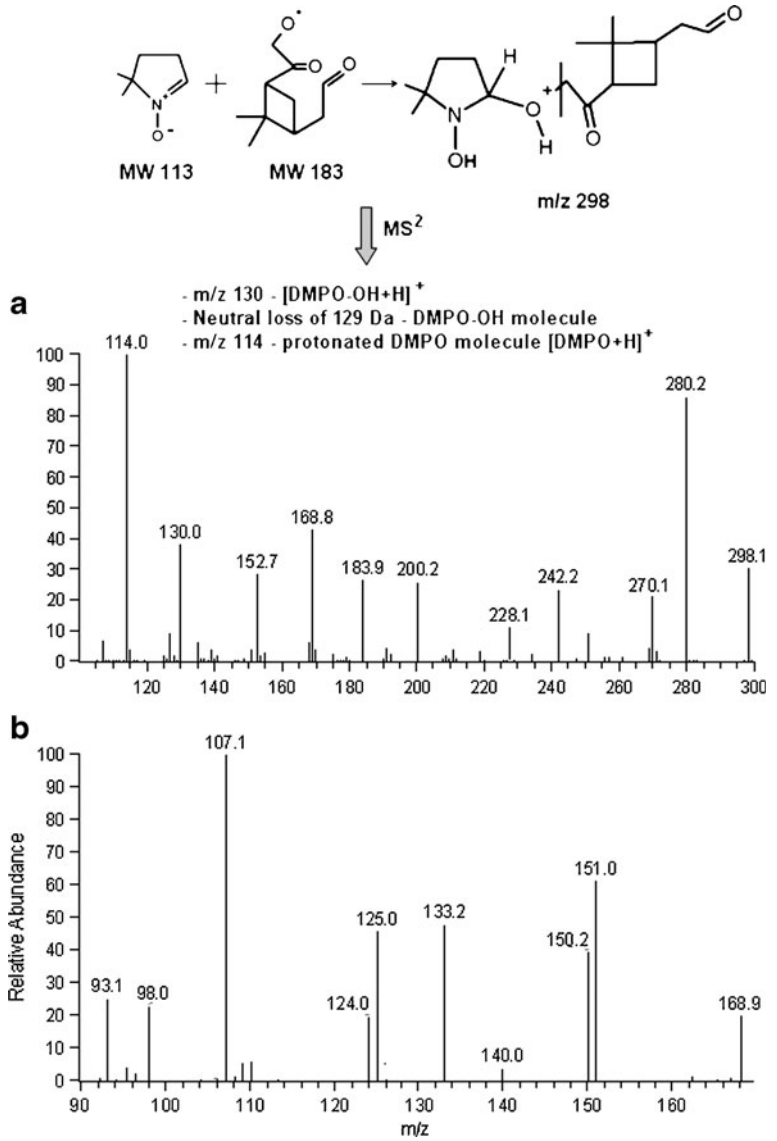

Fig. 4 **a**) Formation and MS^2 fragmentation of DMPO-alkyl adduct at m/z 298 **b**) MS^3 fragmentation of m/z 169

same type of adduct was observed with DMPO at m/z 130. DEPMPO provided further evidence that the captured radical has alkoxyl nature and is bonded to the spin trap via an oxygen atom. These characteristic MS/MS fragments for alkoxyl radical species with DEPMPO were reported in previous free radical studies as well (Reis et al. 2009; Tuccio et al. 2006). Additional fragmentation results are in agreement with the proposed spin trap adduct and RO· structure and are provided in the Supporting Information.

The adduct at m/z 404 (Fig. 2d) had its most abundant fragments showing the loss of water (−18 Da) or diethyl phosphonate molecule (−138 Da). The MS^2 spectrum (shown in

Scheme 4 Proposed fragmentation pathways for the transition m/z 298 → m/z 169

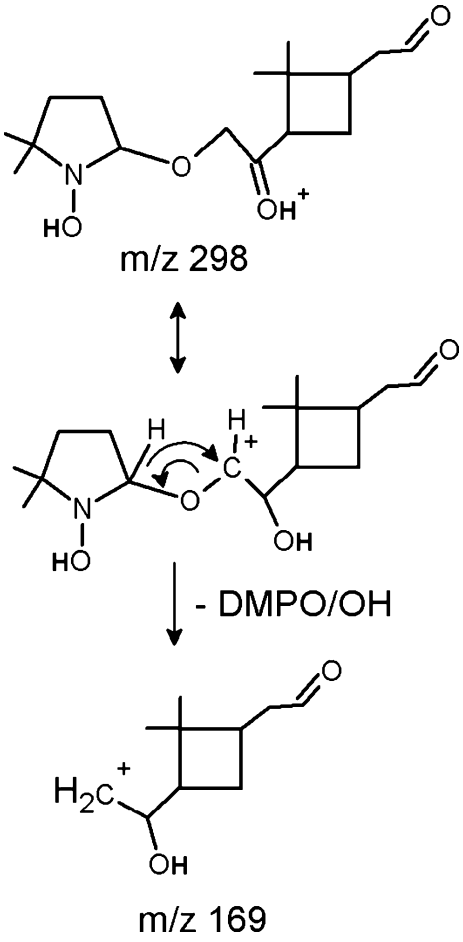

the Supporting Information) also revealed fragments with m/z 236 and m/z 252 that belong to protonated DEPMPO molecule and its protonated hydroxyl adduct, respectively. That fragmentation pattern suggests an alkoxyl (RO·) structure of captured radicals. An ion at m/z 169 that was observed after the loss of DEPMPO molecule (−235 Da) represents the protonated radical specie, i.e. $[ROH+H]^+$ with MW=167.

Under NOx-free conditions (present study), self-reactions of peroxyl (RO_2) radicals can lead to alkoxyl radical formation (Kroll and Seinfeld 2008). The RO radicals are highly reactive and their major removal processes include reaction with oxygen (carbonyl and OOH formation), unimolecular decomposition (alkyl radical and carbonyl formation), and unimolecular isomerization (alkyl radical formation). The rates of these three reactions are a function of temperature and the molecular structure of each individual alkoxyl radical (Atkinson 2007; Atkinson 1997).

3.5 Peroxyl radicals (ROO)

The ions at m/z 314 (adducts of DMPO trap) in Fig. 2b and m/z 436 (adducts of DEPMPO trap) in Fig. 2d are identified as adducts formed with peroxyl oxygen-centered radicals. The

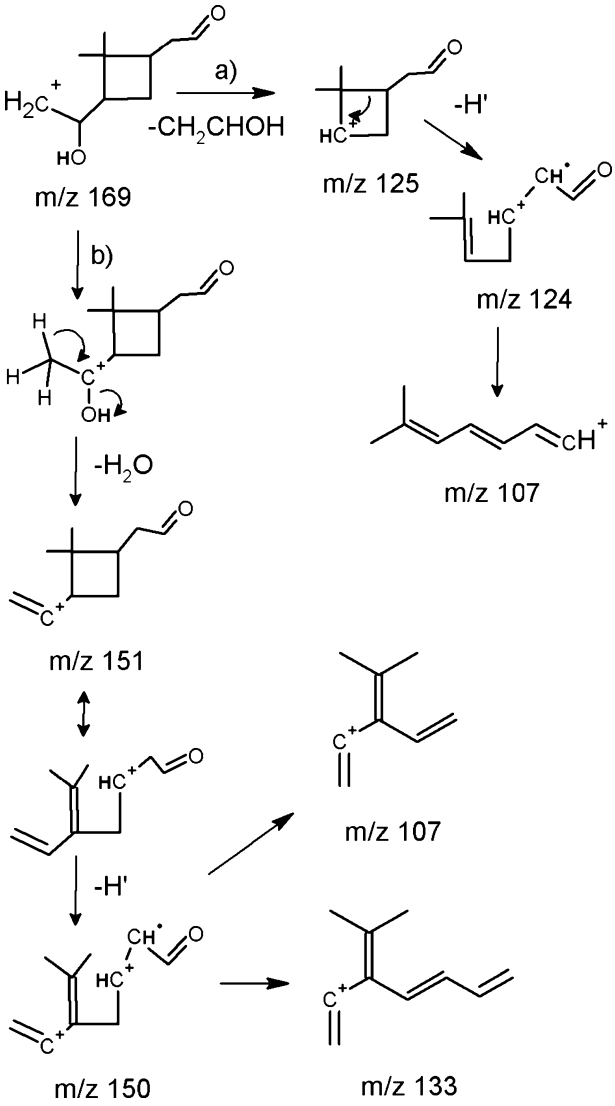

Scheme 5 Proposed fragmentation pathways for the transitions **a**) m/z 169 → m/z 125 → m/z 124 → m/z 107; **b**) m/z 169 → m/z 151 → m/z 150 → m/z 107; 133

formation as well as the fragmentation spectra of adduct at m/z 314, that originates from peroxyl (ROO·) radicals with a molecular weight of 199 Da, is shown in Fig. 5a.

Formation of the fragments at m/z 130 and m/z 114 (DMPO trap) is proposed to occur analogous to the previously described alkoxyl adduct. The ions at m/z 130 suggest that the spin trap molecule is linked to the free radical specie by the oxygen atom. A peroxyl structure of the radical specie captured as the DMPO adduct at m/z 314 is confirmed with MS^2 fragmentation by the presence of m/z 148 ion (Fig. 4a). That ion corresponds to the protonated molecule of the DMPO-hydroperoxyl adduct, $[DMPO\text{-}OOH+H]^+$. An abundant m/z 201 ion, formed by the loss of DMPO (−113 Da) molecule, additionally confirms the formation of the DMPO adduct. A numerous reactions can be involved in that fragment formation and Scheme 6 depicts one of them. Further elimination of one molecule of water

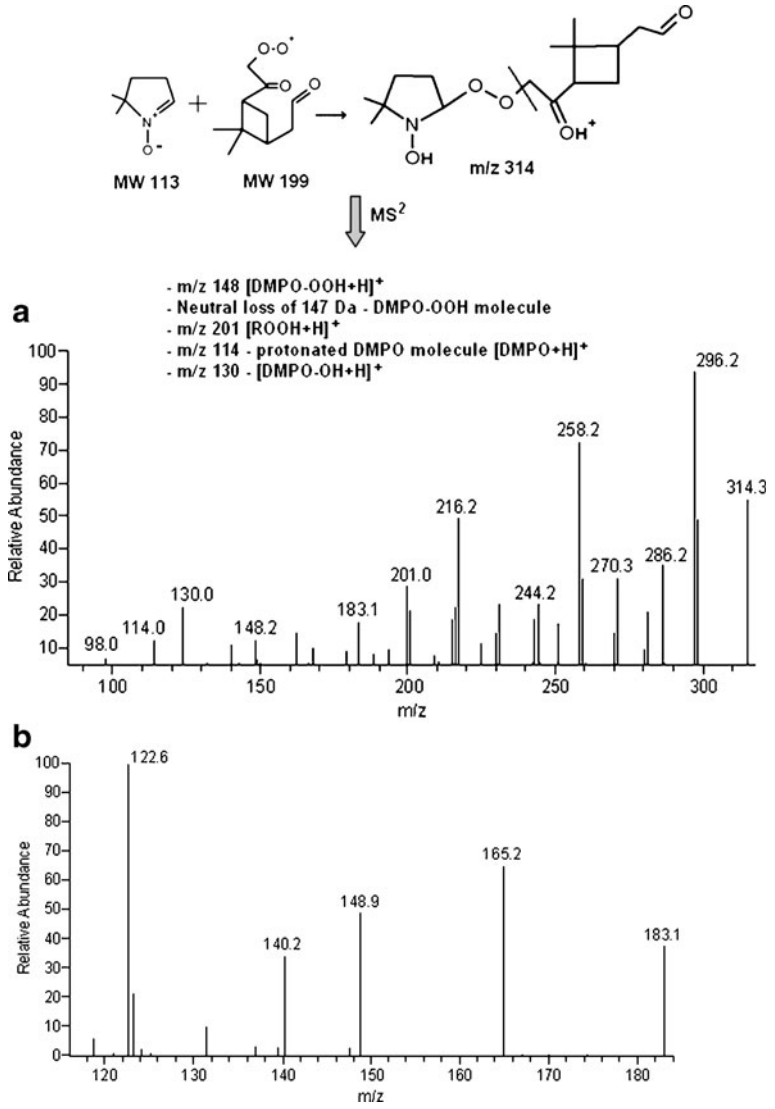

Fig. 5 **a**) Formation and MS^2 fragmentation of DMPO-alkyl adduct at m/z 314 **b**) MS^3 fragmentation of m/z 183

(−18 Da) leads to the formation of ions with m/z 183, with possible hydroperoxyl structure, that will be analyzed later in detail by MS^3 fragmentation.

Other common fragments correspond to the neutral loss of H_2O at m/z 296 (−18 Da), C_2H_4 group at m/z 286 (−28 Da), C_2H_4O group at m/z 270 (−44 Da), C_3H_4O at m/z 258 (−58 Da), C_4H_6O at m/z 244 (−70 Da), and $C_6H_{10}O$ at m/z 216 (−98 Da). These neutral losses were consistent with previous MS^2 results for the ions with m/z 268 and m/z 298 and thus the same fragmentation reactions are proposed here.

In order to further investigate the structure of the proposed peroxyl radical, MS^3 experiments with the product ion at m/z 183 were carried out (Fig. 5b). Neutral loss of

Scheme 6 Proposed fragmentation pathways for the transitions m/z 314 → m/z 201 → m/z 183

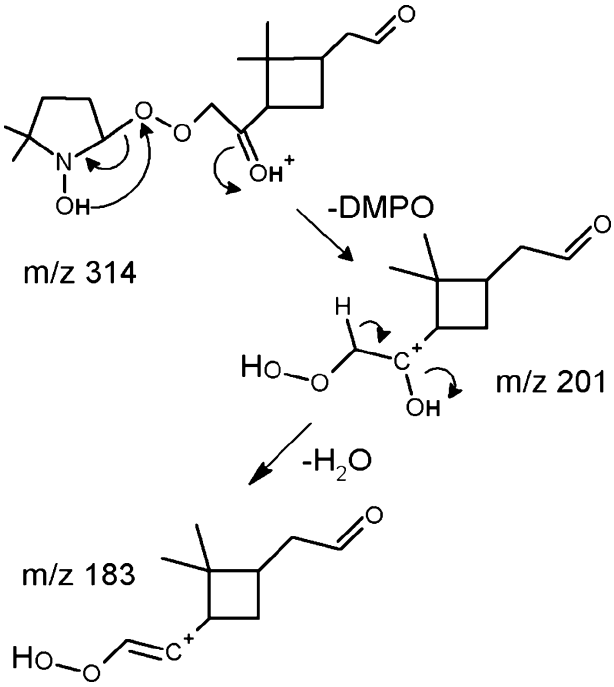

water at m/z 165 can be observed, but more interesting is the presence of fragment with m/z 149 (−34 Da). That significant neutral loss of 34 Da can be explained by the expulsion of H_2O_2 molecule (Scheme 7), and is the indication for the existence of organic hydroperoxides.

Recently, Reinnig and coworkers (2009) identified organic peroxides and hydroperoxy acids in SOA, formed during the ozonolysis of α-pinene and other monoterpenes, by online on-line atmospheric pressure chemical ionization ion trap mass spectrometry (APCI (+) ITMS). That identification is based on a characteristic neutral loss of 34 Da (H_2O_2), which is also observed in the present study, and therefore explains peroxyl nature of captured oxygen radicals.

Scheme 7 Proposed fragmentation pathways for the transition m/z 183 → m/z 149

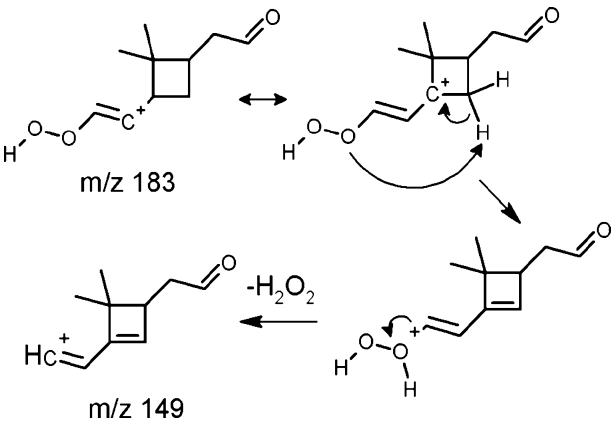

Further evidence for that peroxyl radical (MW 199 Da) is provided by the fragmentation of the DEPMPO adduct with the same radical at m/z 436 (Supporting Information, Fig. 5SP) and an ion at m/z 270. That fragment ion can be the protonated hydroperoxyl-DEPMPO adduct, $[DEPMPO\text{-}OOH+H]^+$. Specific fragments detected in MS^2 spectra of both spin traps and used for peroxyl radical identification in the present study, were observed in previous studies done with the same traps but for different experimental reactions (Reis et al. 2003, 2004, 2009). Those fragments and MS^2 spectra are described in more details in the Supporting Information.

The peroxyl radical detected only in the presence of DEPMPO trap has MW 157 and formed adduct at m/z 394 (Fig. 2d). Fragmentation of that adduct (spectrum shown in the Supporting Information) resulted in ions that belong to the protonated spin trap molecule (m/z 236), the loss of CO group (−28 Da), and the loss of diethyl phosphonate (−138 Da). A positive ion at m/z 270 corresponds to the protonated hydroperoxyl adduct of DEPMPO, i.e. $[DEPMPO\text{-}OOH+H]^+$. That ion confirms the peroxyl (ROO·) nature of this radical. The peak at m/z 159 is formed after the loss of spin trap molecule (−235 Da) and represents a protonated radical specie $[ROOH+H]^+$.

As already described, peroxyl radicals are formed after initial rapid oxidation of the alkyl radicals, and play a key role in further radical formation. Peroxyl radicals can be either stabilized by H-atom abstraction and form low-volatile hydroperoxides, or undergo self-reactions and form alkoxyl radicals (NOx-free conditions).

4 Conclusions

The oxidative properties of the α-pinene/ozone reaction products were studied by the $ESI(+)/MS^n$ in the presence of DMPO or DEPMPO, focusing on the structural identification of reactive radical species. Adducts formed with DEPMPO have longer stability: ~30 min vs. ~15 min with DMPO. Tandem mass spectrometry applied to elucidate structures of radical species from α-pinene ozonolysis, captured in the spin trap adducts, confirmed very low structural differences among them. Differences that exist are characterized either by the absence or presence of oxygen, bonded to the spin trap molecule (carbon- or oxygen- centered radicals, respectively). A characteristic MS^2 fragments at m/z 114, m/z 130, and m/z 148 in the presence of DMPO, and m/z 236, m/z 252, and m/z 270 (Scheme 8) in the presence of DEPMPO are indication for the existence of alkyl, alkoxyl and peroxyl radicals, respectively.

During the α-pinene ozonolysis a number of intermediate species are formed, some of which are reactive radicals. Proposed formation of two identified carbon- (MW 153 and 125 Da) and four oxygen-centered radicals (MW 157, 167, 183, and 199 Da) is illustrated in Fig. 6. The detection and identification of radicals with molecular weights 199, 183, 153, and 167 Da supported the mechanism and structure suggestions previously implied by Winterhalter and co-workers (2003). A possible reaction mechanism leading to the formation of detected radicals with masses 125 and 157 Da has been reported for first time.

With the approach presented here, it is possible to more precisely characterize products from the α-pinene/ozone reaction and finally provide an indication for the existence of reactive radicals. However, a concern that arises from the present study is “longer than expected” atmospheric life time of unstable radical species. Less likely, the presence of unstable radicals in the particulate phase can be explained by classic gas-particle partitioning theory, since this partitioning will be affected by high chemical reactivity of radicals and high oxygen concentration in the flow system. For example, the simplest acyl radicals (CH_3CO and

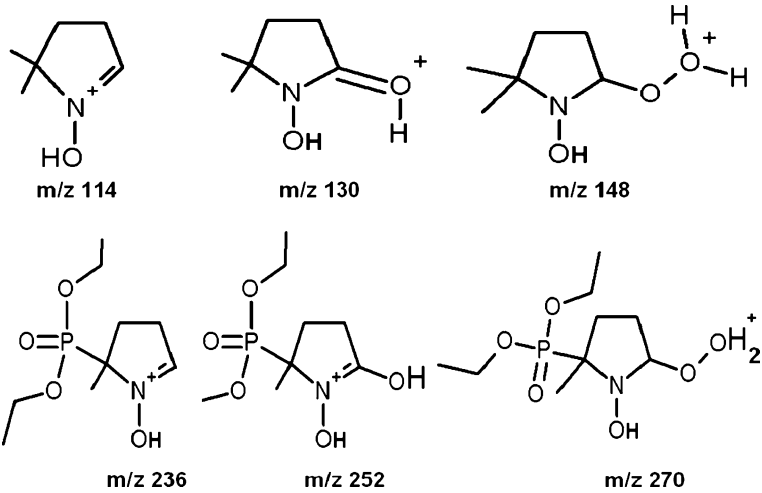

Scheme 8 Structures of DMPO (m/z 114, m/z 130, and m/z 148) and DEPMPO (m/z 236, m/z 252, and m/z 268) fragments

C_2H_5CO) react with O_2 with reaction rate at the order of 10^{-13}–10^{-12} cm^3 $molecule^{-1}$ s^{-1} and the simplest alkoxyl radicals (CH_3O and C_2H_5O) react with O_2 with reaction rate at the order of 10^{-14} cm^3 $molecule^{-1}$ s^{-1}. One possible explanation might be that the radicals are very rapidly taken up by the particles and not further exposed to oxygen. In addition, some stable organic species upon gas-particle partitioning can undergo further reactions in the particle phase and form unstable radical products that will be captured by nitrone spin traps. The theoretical possibility about continuing chemistry in the particle phase has been described in more detail in the review by Kroll and Seinfeld (2008), which focuses specifically on the chemistry of SOA formation. All organic particle-phase compounds are susceptible to

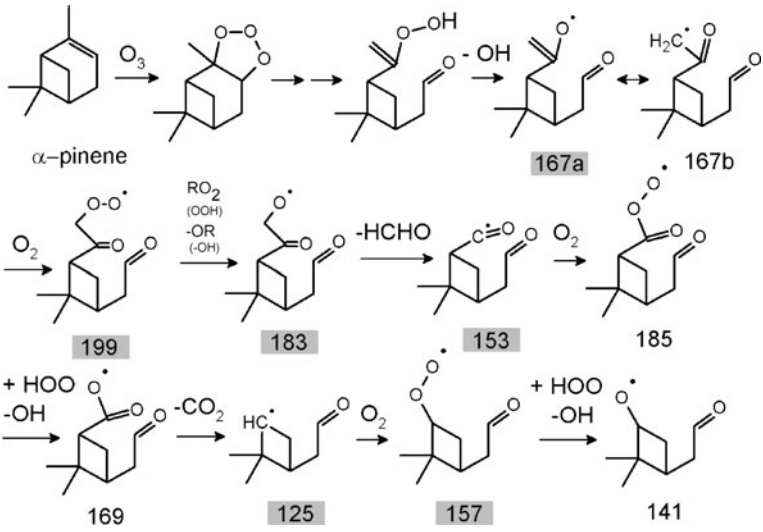

Fig. 6 Proposed gas-phase reaction mechanism of α-pinene and ozone leading to the formation of detected radicals

oxidation by other oxidative species and radicals (OH, OOH, R, RO, ROO) and that suggested framework can also provide a reasonable explanation for detection of short-life radicals in the particle phase in the present study.

If the identified radicals are formed from the first-generation reactions (standard gas-phase chemistry), then the structures and reactions presented in Fig. 6 illustrate possible radical structures and their formation pathways. However, if the radicals are formed from the higher-generation reactions (continuing particle phase chemistry), then their structures could be different than shown in Fig. 6. The definite formation pathways leading to the observed products in the particulate phase remain speculative at present.

In general, this study provided initial evidence for the presence of alkyl, alkoxyl, and peroxyl radicals in the particulate phase from the monoterpene/ozone reaction, proposed its structures, and the reactions leading to their formation. More studies should be done in the same field with ultra-high resolution mass spectrometry to accurately define mass (and elemental composition) of detected radical species. In order to make the method more real-time, and to capture radical species in nitrone adducts immediately during collection, particle-into-liquid-sampler (PILS) should be used.

Acknowledgments This work was supported by U.S Environmental Protection Agency's Science to Achieve Results (STAR) Program through a subcontract from the University of Rochester PM and Health Center Grant RD832415. Although the research described in this article has been funded wholly or in part by the United States Environmental Protection Agency, it has not been subjected to the Agency's peer and policy review and therefore, does not necessarily reflect the views of the Agency and no official endorsement should be inferred.

References

Aschmann, S.M., Arey, J., Atkinson, R.: OH radical formation from the gas-phase reactions of O_3 with a series of terpenes. Atmos. Environ. **36**, 4347–4355 (2002)

Atkinson, R.: Atmospheric reactions of alkoxy and β-hydroxyalkoxy radicals. Int. J. Chem. Kin. **29**, 99–111 (1997)

Atkinson, R.: Rate constants for the atmospheric reactions of alkoxy radicals: An updated estimation method. Atmos. Environ. **41**, 8468–8485 (2007)

Atkinson, R., Tuazon, E.C., Aschmann, S.M.: Products of the gas-phase reactions of O_3 with alkenes. Environ. Sci. Technol. **29**, 1860–1866 (1995)

Chen, X., Hopke, P.K.: Secondary organic aerosol from α-pinene ozonolysis in dynamic chamber system. Indoor Air **19**, 335–345 (2009a)

Chen, X., Hopke, P.K.: A chamber study of secondary organic aerosol formation by linalool ozonolysis. Atmos. Environ. **43**, 3935–3940 (2009b)

Chen, X., Hopke, P.K.: A chamber study of secondary organic aerosol formation by limonene ozonolysis. Indoor Air **20**, 320–328 (2010)

Chen, X., Hopke, P.K., Carter, W.P.L.: Secondary organic aerosol from ozonolysis of biogenic volatile organic compounds: chamber studies of particle and reactive oxygen species formation. Environ. Sci. Technol. **45**, 276–282 (2011)

Delfino, R.J., Sioutas, S., Malik, S.: Potential role of ultrafine particles in associations between airborne particle mass and cardiovascular health. Environ. Health Perspect. **113**, 934–946 (2005)

Domingues, P., Domingues, M.R.M., Amado, F.M.L., Ferrer-Correia, A.J.: Detection and characterization of hydroxyl radical adducts by mass spectrometry. Am. Soc. Mass Spectrom. **12**, 1214–1219 (2001)

Domingues, M.R.M., Domingues, P., Reis, A., Fonseca, C., Amado, F.M.L., Ferrer-Correia, A.J.V.: Identification of oxidation products and free radicals of tryptophan by mass spectrometry. Am. Soc. Mass Spectrom. **14**, 406–416 (2003)

Dreher, D., Junod, A.F.: Role of oxygen free radicals in cancer development. Eur. J. Cancer **32A**, 30–38 (1996)

Glasius, M., Duane, M., Larsen, B.R.: Analysis of polar terpene oxidation products in aerosols by liquid chromatography ion trap mass spectrometry (MS^n). J. Chromatogr. **833**, 121–135 (1999)

Guo, Q., Qian, S.Y., Mason, R.P.: Separation and identification of DMPO adducts of oxygen-centered radicals formed from organic hydroperoxides by HPLC-ESR, ESI-MS and MS/MS. Am. Soc. Mass Spectrom. **14**, 862–871 (2003)

Hallquist, M., Wenger, J.C., Baltensperger, U., Rudich, Y., Simpson, D., Claeys, M., Dommen, J., Donahue, N.M., George, C., Goldstein, A.H., Hamilton, J.F., Herrmann, H., Hoffmann, T., Iinuma, Y., Jang, M., Jenkin, M., Jimenez, J.L., Kiendler-Scharr, A., Maenhaut, W., McFiggans, G., Mentel, T.F., Monod, A., Prevot, A.S.H., Seinfeld, J.H., Surrat, J.D., Szmigielski, R., Wildt, J.: The formation, properties and impact of secondary organic aerosol: current and emerging issues. Atmos. Chem. Phys. **9**, 5155–5236 (2009)

Kroll, J.H., Seinfeld, J.H.: Chemistry of secondary organic aerosol: formation and evolution of low-volatility organics in the atmosphere. Atmos. Environ. **42**, 3593–3624 (2008)

Li, N., Sioutas, C., Cho, A., Schmitz, D., Misra, C., Sempf, J., Wang, M., Oberley, T., Froines, J., Nel, A.: Ultrafine particulate pollutants induce oxidative stress and mitochondrial damage. Environ. Health Perspect. **111**(4), 455–460 (2003a)

Li, N., Hao, M., Phalen, R.F., Hinds, W.C., Nel, A.E.: Particulate air pollutants and asthma. A paradigm for the role of oxidative stress in PM-induced adverse health effects. Clin. Immunol. **109**, 250–265 (2003b)

Pope, C.A., Dockery, D.W.: Health effects of fine particulate air pollution: Lines that connect. J Air Waste Manag Assoc. **56**, 709–742 (2006)

Pope, C.A., Burnett, R.T., Thun, M.J., Calle, E.E., Krewski, D., Ito, K., Thurston, G.D.: Lung cancer, cardiopulmonary mortality, and long-term exposure to fine particulate air pollution. J. Am. Med. Assoc. **287**, 1132–1141 (2002)

Reinnig, M., Warnke, J., Hoffmann, T.: Identification of organic hydroperoxides and hydroperoxy acids in secondary organic aerosol formed during the ozonolysis of different monoterpenes and sesquiterpenes by on-line analysis using atmospheric pressure chemical ionization ion trap mass spectrometry. Rapid Commun. Mass Spectrom. **23**, 1735–1741 (2009)

Reis, A., Domingues, M.R.M., Amado, F.M.L., Ferrer-Correia, A.J.V., Domingues, P.: Detection and characterization by mass spectrometry of radical adducts produced by linoleic acid oxidation. Am Soc Mass Spectrom **14**, 1250–1261 (2003)

Reis, A., Domingues, P., Ferrer-Correia, A.J.V., Domingues, M.R.M.: Identification by tandem mass spectrometry of spin-trapped free radicals from oxidized 2-oleoyl-1-palmitoyl-*sn*-glycero-3-phosphocholine. Rapid Commun. Mass Spectrom. **18**, 1047–1058 (2004)

Reis, A., Domingues, M.R.M., Oliveira, M.M., Domingues, P.: Identification of free radicals by spin trapping with DEPMPO and MCPIO using tandem mass spectrometry. Eur. J. Mass Spectrom. **15**, 689–703 (2009)

Tolocka, M. P., Jang, M., Ginter, J.M., Cox, F.J., Kamens, R.M., Johnston, M.V.: Formation of oligomers in secondary organic aerosol. Env. Sci. & Tech. **38**, 1428–1434 (2004)

Tuccio, B., Lauricella, R., Charles, L.: Characterization of free radical spin adducts of the cyclic β-phosphorylated nitrone DEPMPO using tandem mass spectrometry. Int. J. Mass Spectrom. **252**, 47–53 (2006)

Venkatachari, P., Hopke, P.K., Grover, B.D., Eatough, D.J.: Measurement of particle-bound reactive oxygen species in Rubidoux aerosols. J. Atmos Chem. **50**, 49–58 (2005)

Venkatachari, P., Hopke, P.K.: Development and evaluation of a particle-bound reactive oxygen species generator. J. Aerosol Sci. **39**, 168–174 (2008)

Venkatachari, P., Hopke, P.K., Brune, V.H., Ren, X., Lesher, R., Mao, J., Mitchell, M.: Characterization of wintertime reactive oxygen species concentrations in Flushing, New York. Aerosol Sci. Technol. **41**, 97–111 (2007)

Winterhalter, R., Dingenen, R.V., Larsen, B.R., Jensen, N.R., Hjorth, J.: LC-MS analysis of aerosol particles from the oxidation of α-pinene by ozone and OH-radicals. Atmos. Chem. Phys. Discuss. **3**, 1–39 (2003)

Wolkoff, P., Clausen, P.A., Jensen, B., Nielsen, G.D., Wilkins, C.K.: Are we measuring the relevant indoor pollutants? Indoor Air **7**, 92–106 (1997)